Electronic Supplementary Material (ESI) for Inorganic Chemistry Frontiers.

Supplementary Information

Ni/Ni_3C core-shell nanoparticles encapsulated in N-doped bamboo-like carbon nanotubes towards efficient overall water splitting

Tao Dong,[a] Xiao Zhang,[b] Yongqiang Cao[a], Hsueh-Shih Chen[c] and Ping Yang[a*]

[a] School of Material Science and Engineering, University of Jinan, Jinan 250022, P. R. China.

[b] Fuels and Energy Technology Institute and Department of Chemical Engineering, Curtin University, Perth WA6845, Australia.

[c] Department of Materials Science & Engineering, National Tsing Hua University, Hsinchu City 300, Taiwan

*Corresponding Author has to be addressed.E-mail address: mse_yangp@ujn.edu.cn (P. Yang)

Turn-over frequency (TOF)

We used the following formula to calculate the TOF [1]:

$$TOF = \frac{\#total\ hydrogen\ turn\ overs\ /\ cm^2\ of\ geometric\ area}{\#active\ sites\ /\ cm^2\ of\ geometric\ area}$$

The total number of hydrogen turn overs was calculated from the current density according to:

$$\#\ H_2 = \left(j\ \frac{mA}{cm^2}\right)\left(\frac{1\ C\ s^{-1}}{1000\ mA}\right)\left(\frac{1\ mol\ e^-}{96458.3\ C}\right)\left(\frac{1\ mol\ H_2}{2\ mol\ e^-}\right)\left(\frac{6.022 \times 10^{23}\ H_2\ molecules}{1\ mol\ H_2}\right) = per\ \frac{mA}{cm^2}$$

The active site per real surface area is calculated from the following formula:

The molar volume of Ni:

$$V_m = \frac{F_w}{\rho} = \frac{58.69\ g/mol}{8.9\ g/cm^3} = 6.594 \frac{cm^3}{mol_{Ni}}$$

The average surface occupancy:

Active site number of Ni

$$= \left(\frac{1\ atoms/formula\ unit}{\frac{6.594\ cm^3/mol_{Ni}}{6.022 \times 10^{23}\ mol^{-1}}}\right)^{2/3} = 2.03 \times 10^{15}\ surface\ atoms\ /\ cm^2$$

The molar volume of Ni_3C:

$$V_m = \frac{F_w}{\rho} = \frac{188.4\ g/mol}{7.85\ g/cm^3} = 23.698 \frac{cm^3}{mol_{Ni_3C}}$$

The average surface occupancy:

Active site number of Ni_3C

$$= \left(\frac{3\ atoms/formula\ unit}{\frac{23.698\ cm^3/mol_{Ni}}{6.022 \times 10^{23}\ mol^{-1}}}\right)^{2/3} = 1.8 \times 10^{15}\ surface\ atoms\ /\ cm^2$$

We estimate the number of active sites as the number of surface sites from the average value of Ni and Ni_3C.

Active site number $= 1.915 \times 10^{15}\ surface\ atoms\ /\ cm^2$

TOF can be calculated according to:

$$TOF = \frac{(3.12 \times 10^{15} \frac{H_2/s}{cm^2} per \frac{mA}{cm^2}) \times |j|}{\#active\ sites\ \times\ A_{ECSA}}$$

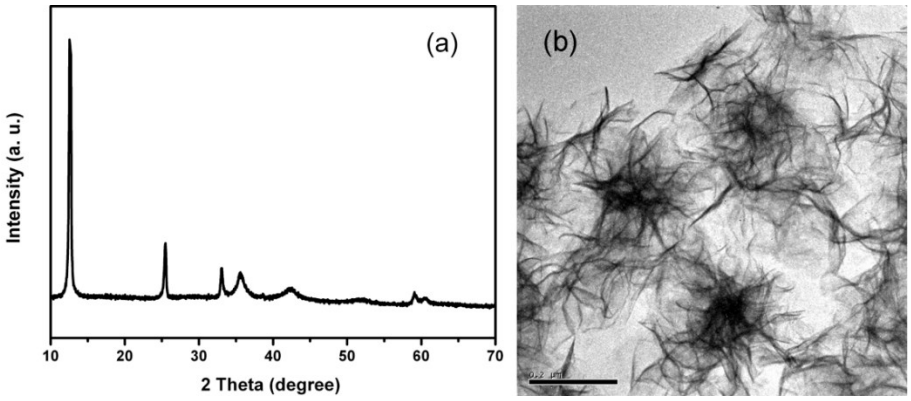

Fig. S1 (a) XRD pattern and (b) TEM image of sample $Ni(OH)_2$.

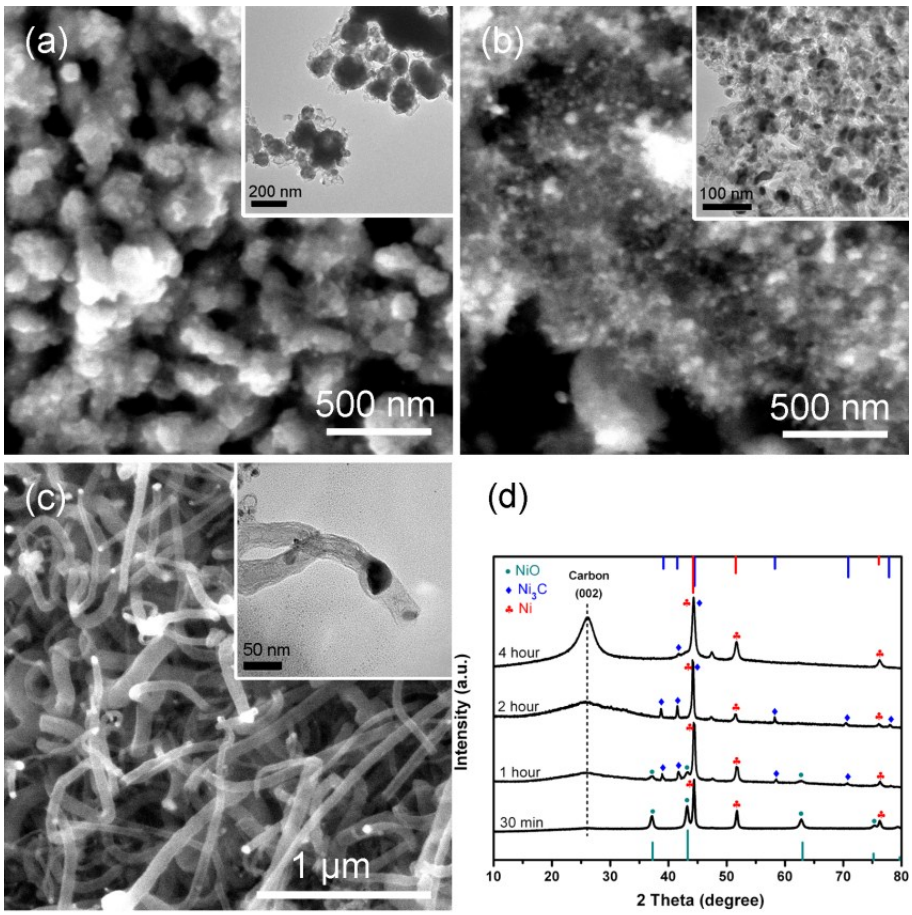

Fig. S2 SEM and TEM images of samples prepared by different annealing time: (a) 0.5h, (b) 1h, (c) 4h. (d) XRD patterns of samples prepared by different annealing time.

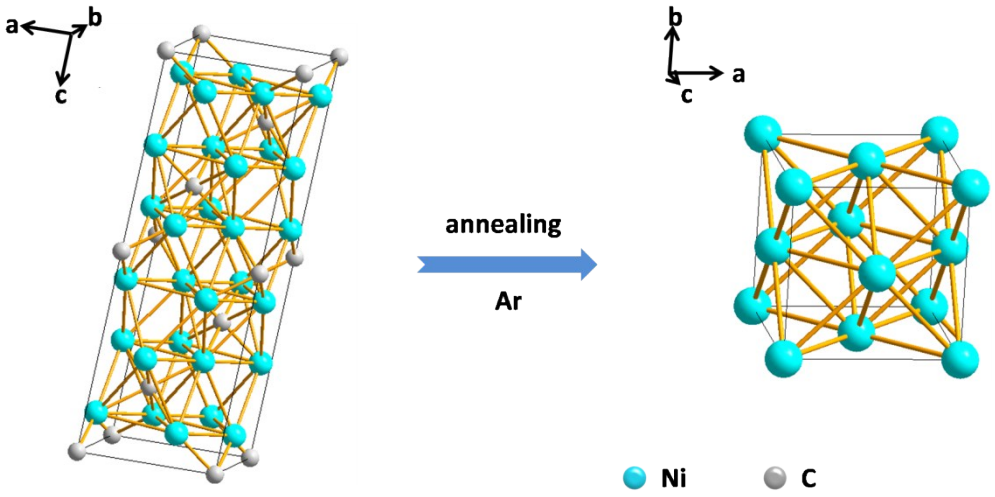

Fig. S3 Crystal structure models of trigonal Ni_3C and cubic Ni, and their phase transformation by annealing.

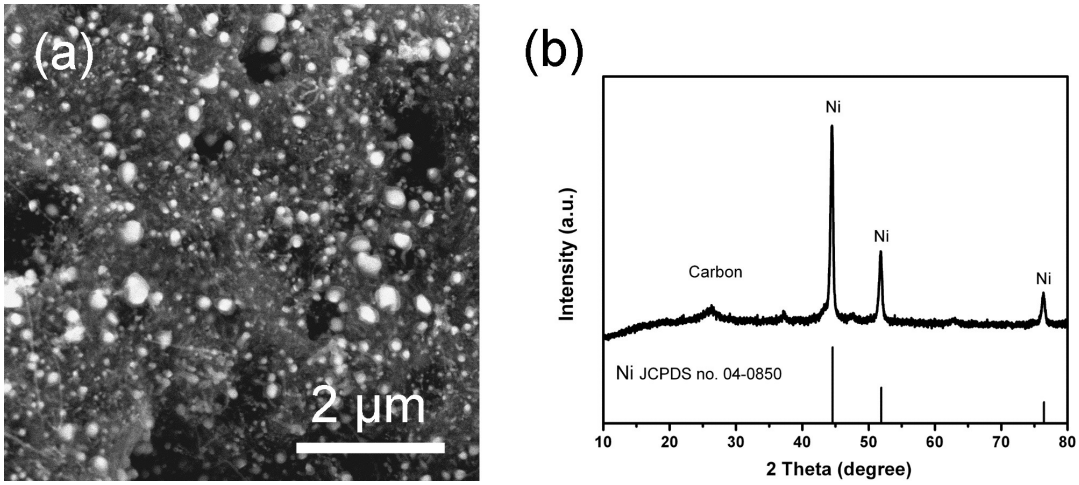

Fig. S4 (a) SEM image and (b) XRD pattern of sample prepared with nickel nitrate and Dicyandiamide.

In detail, 30 mg of $Ni(NO_3)_2 \cdot 6H_2O$ and 200 mg of dicyandiamide were ground in a mortar with ethanol for uniform mixing. After the mixture were dried at 60 °C, the solid powders were placed in a covered crucible and annealed at 650 °C for 2 hours under an argon atmosphere, the heating rate is 5 °C/min.

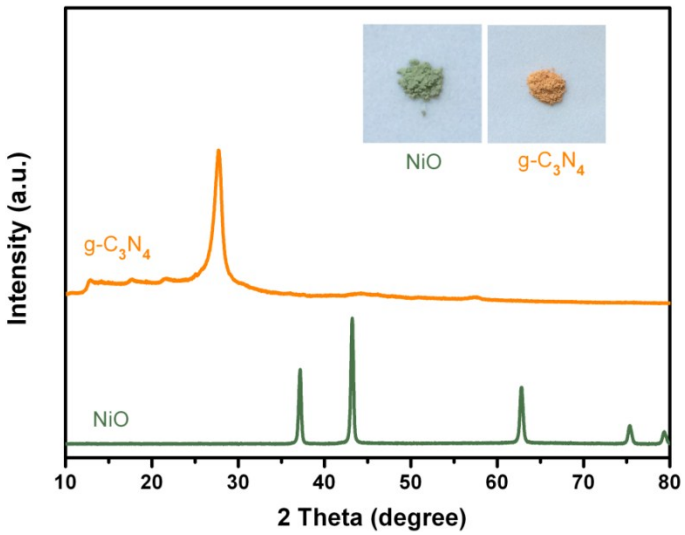

Fig. S5 XRD patterns of the products prepared by annealing of single dicyandiamide or $Ni(OH)_2$, inserts show the photographs.

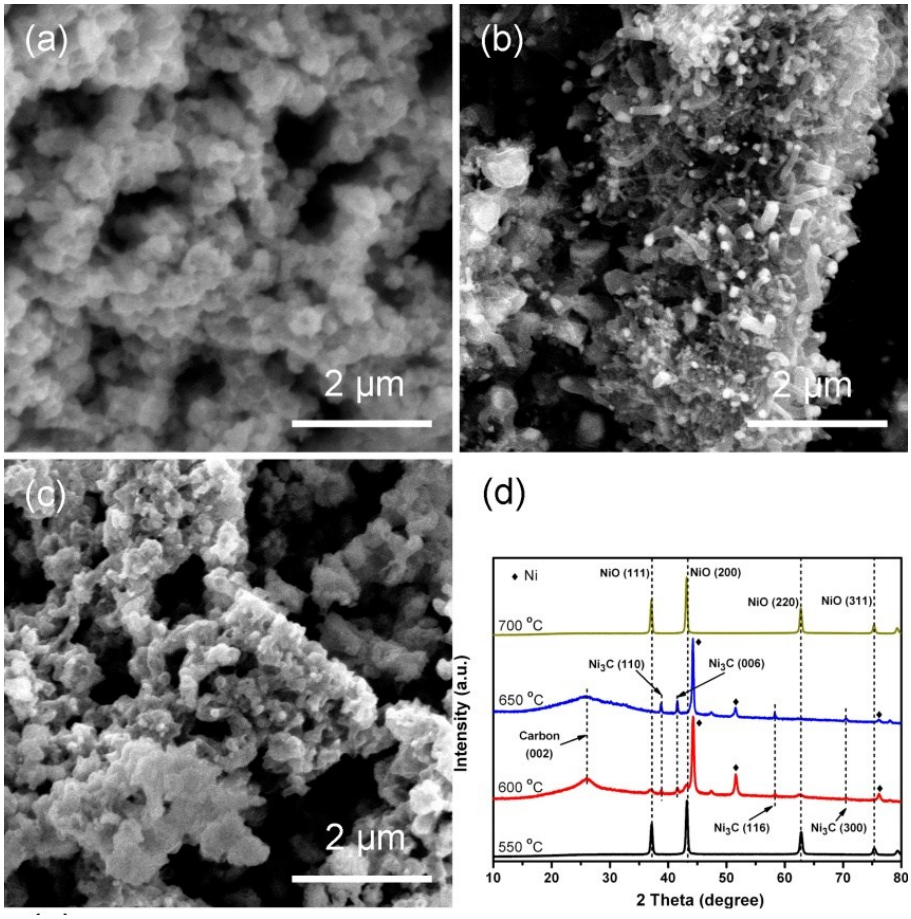

Fig. S6 SEM and TEM images of samples prepared by different annealing temperature for 2 h: (a) 550 °C, (b) 600 °C, (c) 700 °C. (d) XRD patterns samples prepared by different annealing temperature.

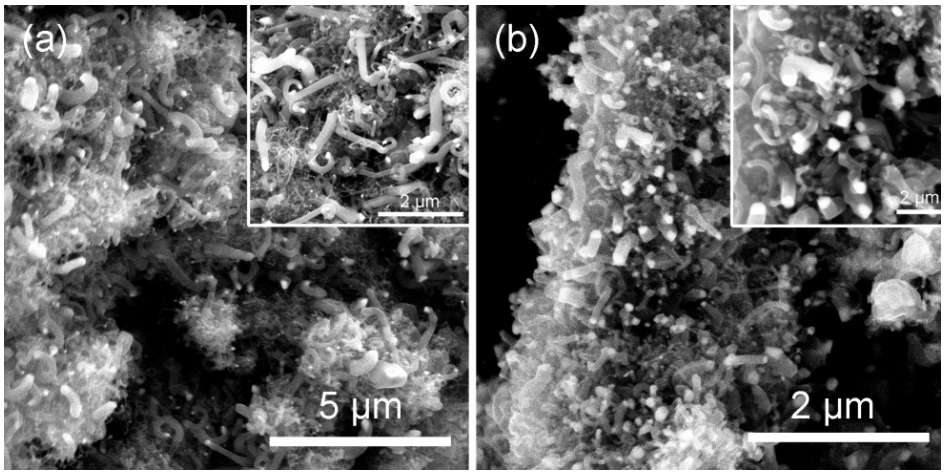

Fig. S7 SEM images of samples prepared by different amounts of dicyandiamide: (a) 100 mg, (b)

400 mg.

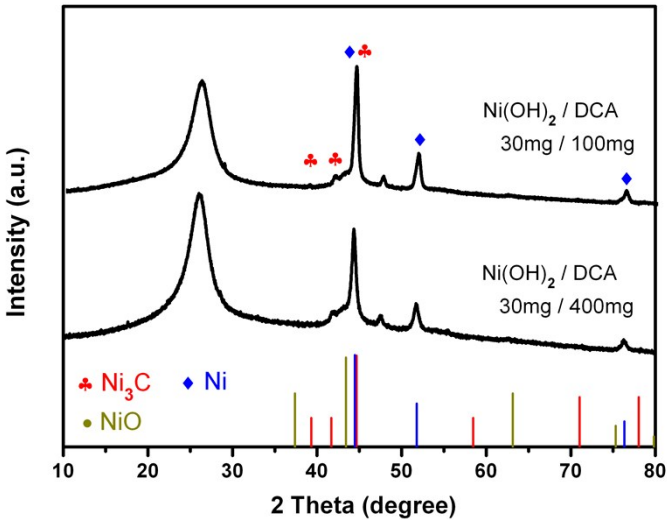

Fig. S8 XRD patterns of samples prepared by different amounts of dicyandiamide.

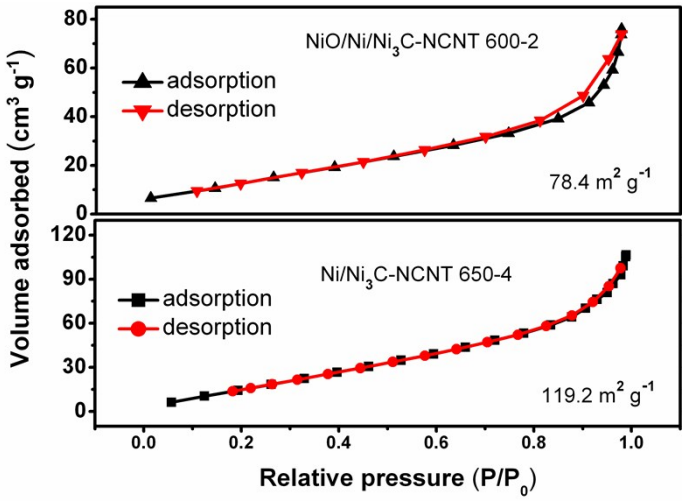

Fig. S9 N_2 adsorption/desorption isotherms of Ni/Ni_3C-NCNT 650-4 and $NiO/Ni/Ni_3C$-NCNT 600-2.

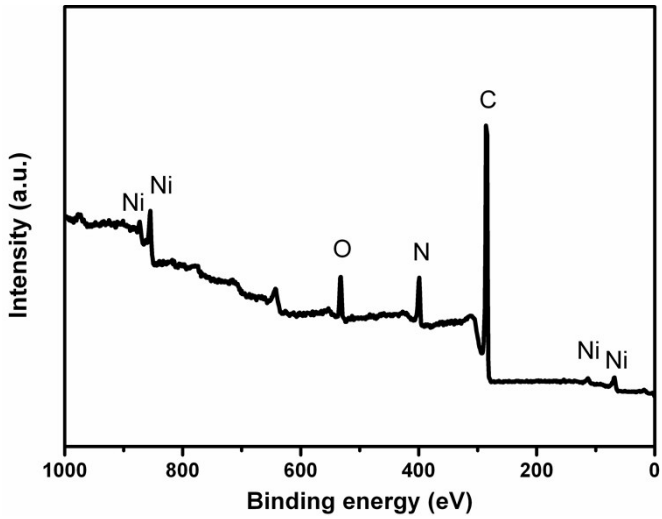

Fig. S10 XPS survey spectrum of Ni/Ni_3C-NCNT 650-2.

Table S1 Percentage of different N species.

N species	Ni-N	Pyridinic-N	Pyrollic-N	Graphitic-N
Percentage (%)	8.69	64.82	20.59	5.91

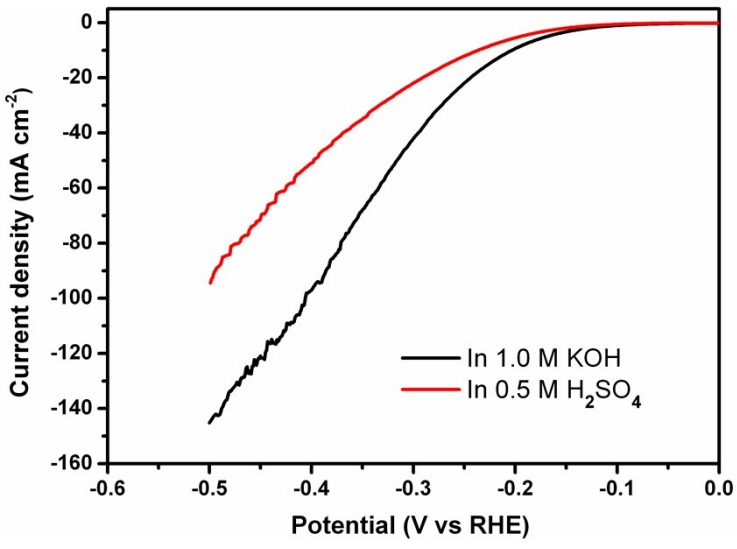

Fig. S11 LSV polarization curves of Ni/Ni_3C-NCNT 650-2 for HER in acidic or alkaline solution.

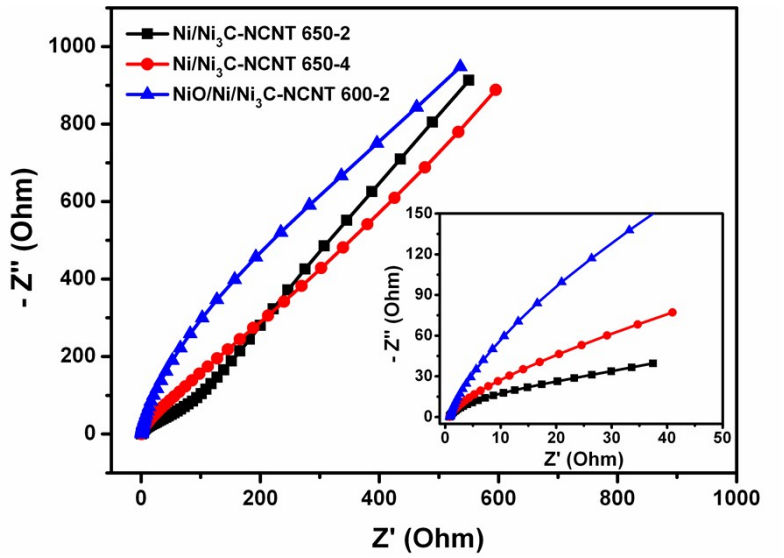

Fig. S12 EIS plots of Ni/Ni_3C-NCNT 650-2, Ni/Ni_3C-NCNT 650-4 and NiO/Ni/Ni_3C-NCNT 600-2.

Table S2 Comparison of HER performance of the Ni/Ni_3C-NCNT 650-2 with other non-noble-metal catalysts in 1.0 M KOH solution.

Electrocatalysts	Overpotential (mV)(j=10 mA cm^{-2})	Ref.
Ni/Ni_3C-NCNT 650-2	204	This work
CoO_x@CN	270	[2]
MoS_{2+x}/FTO	310	[3]
CoP/CC	209	[4]
Ni_3N	208	[5]
CoP/rGO-400	340	[6]
NiFe-LDH/NF	250	[7]
FeP/Fe foil	194	[8]
Ni_5P_4 nanosheets on Ni foil	150	[9]
Ni_3S_2/NF	223	[10]
Ni_3S_2 nanorod/NF	200	[11]
NiS/NF	158	[12]
$NiCo_2O_4$/NF	164	[13]

Fe-Ni_3C-2%@NCS	178	[14]
Zn-Co-S/CFP	234	[15]
Ni_3FeN/carbon cloth	105	[16]

Table S3 Comparison of OER performance of the Ni/Ni_3C-NCNT 650-2 with other non-noble-metal catalysts in 1.0 M KOH solution.

Electrocatalysts	Overpotential (mV) (j=10 mA cm^{-2})	Ref.
Ni/Ni_3C-NCNT 650-2	277	This work
N doped CNT	450	[17]
N-doped graphite	380	[18]
NiCo LDH	367	[19]
CoZn-NC-700	390	[20]
Ni_3C/C	330	[21]
Ni/Mo_2C-PC	386	[22]
Fe-Ni_3C-2%@NCS	275	[14]
MoS_2-Ni_3S_2 HNRs/NF	249	[23]
$Co_6Mo_6C_2$/NCRGO	260	[24]
Fe-Ni oxide	>375	[25]
$NiCo_2O_4$ NNs/FTO	565	[26]
β-$Ni(OH)_2$	444	[27]
NiOOH	525	[28]
NiO	>470	[29]
TiN@Ni_3N	350	[30]

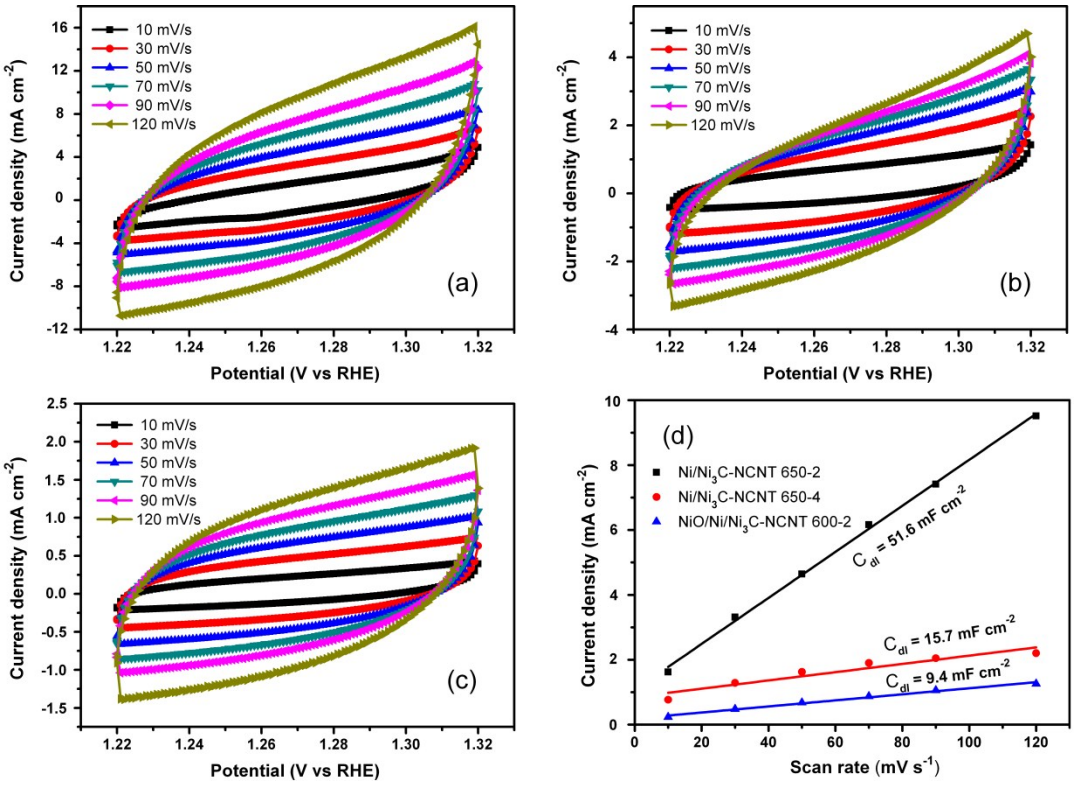

Fig. S13 CV curves of catalysts at various scan rates in the region of 1.22-1.32 V vs RHE: (a) Ni/Ni_3C-NCNT 650-2, (b) Ni/Ni_3C-NCNT 650-4, (c) $NiO/Ni/Ni_3C$-NCNT 600-2. (d) Estimation of C_{dl} by plotting the current density differences ($\Delta j = j_a - j_c$) at 1.27 V with various scan rates.

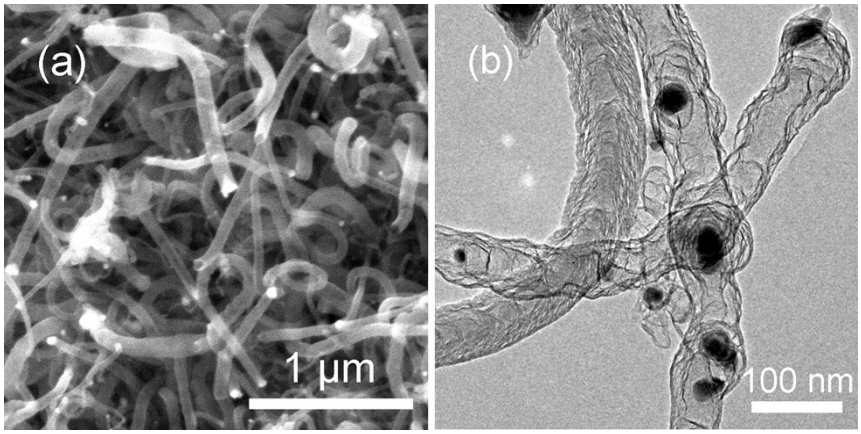

Fig. S14 (a) SEM and (b) TEM images of Ni/Ni_3C-NCNT 650-2 after continuous HER test.

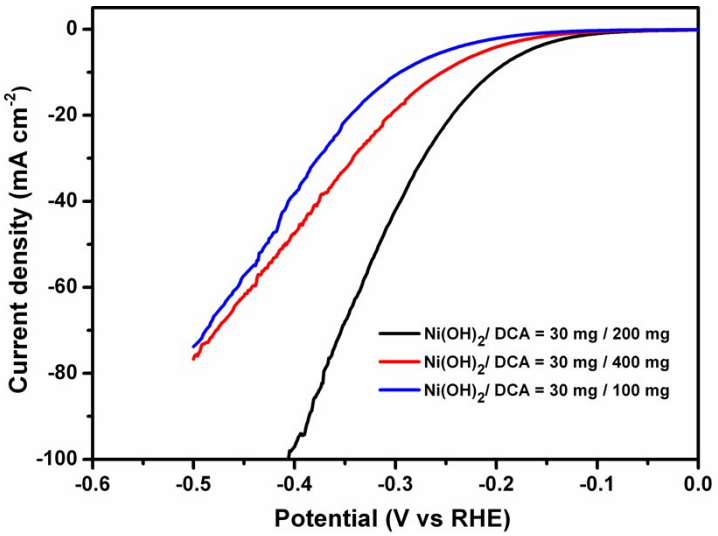

Fig. S15 LSV polarization curves of various catalysts obtained with different amount of dicyandiamide for HER test.

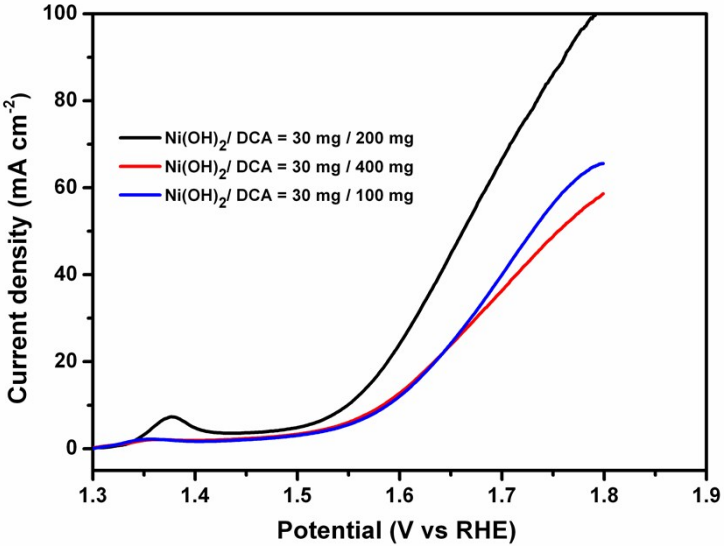

Fig. S16 LSV polarization curves of various catalysts obtained with different amount of dicyandiamide for OER test.

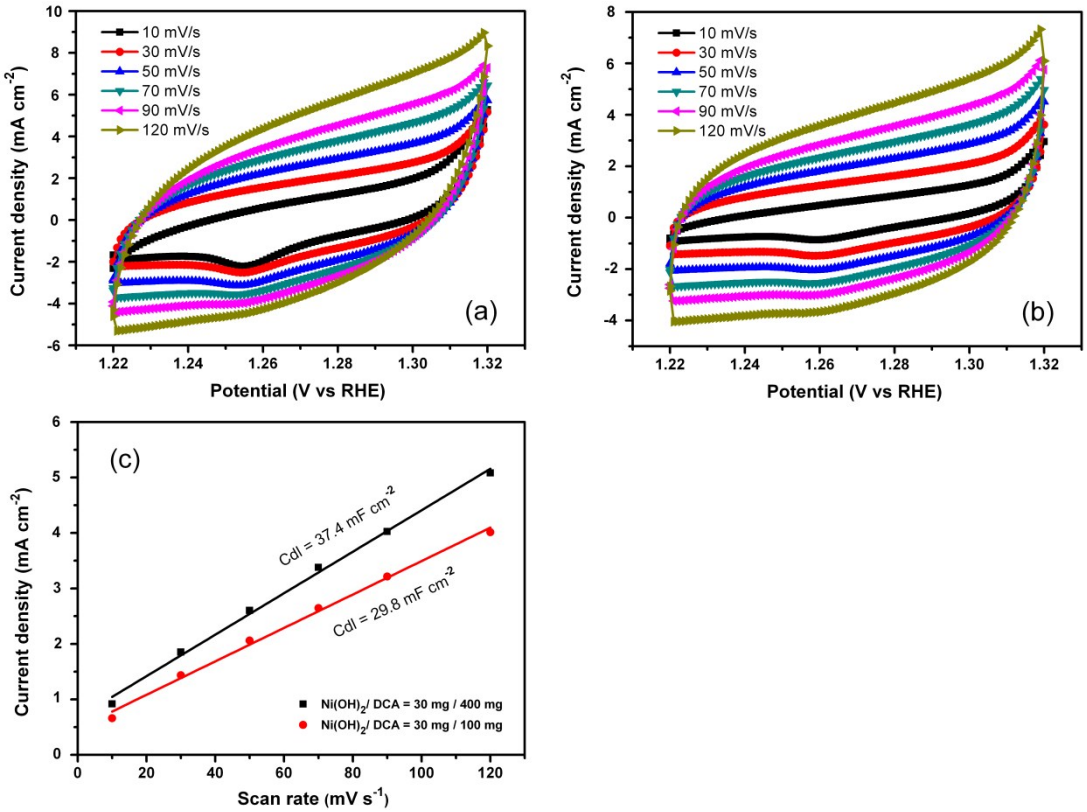

Fig. S17 CV curves of catalysts obtained with different amount of dicyandiamide at various scan rates in the region of 1.22-1.32 V vs RHE: (a) 400mg, (b) 100mg. (c) Estimation of C_{dl} by plotting the current density differences ($\Delta j = j_a - j_c$) at 1.27 V with various scan rates.

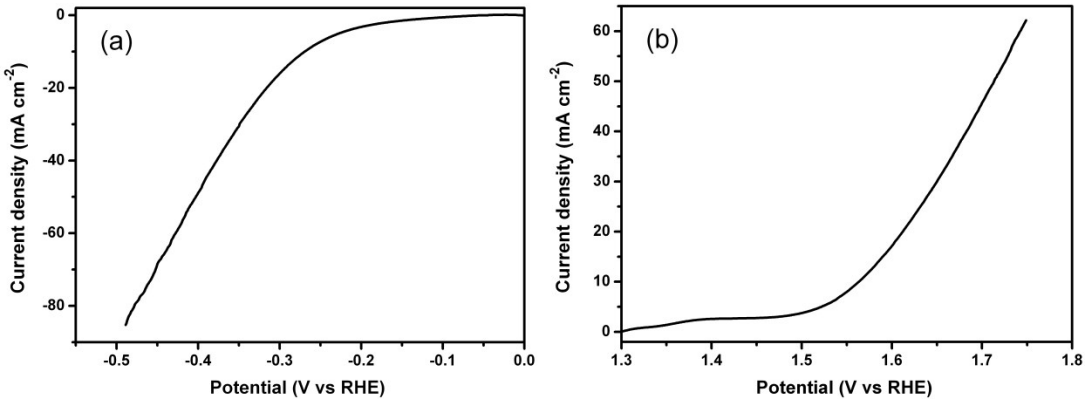

Fig. S18 LSV curves of the product prepared by Nickel nitrate and Dicyandiamide (a) HER and (b) OER.

The overpotentials are 269 mV and 330 mV to reach current density of 10 mA cm^{-2} for HER and OER, respectively.

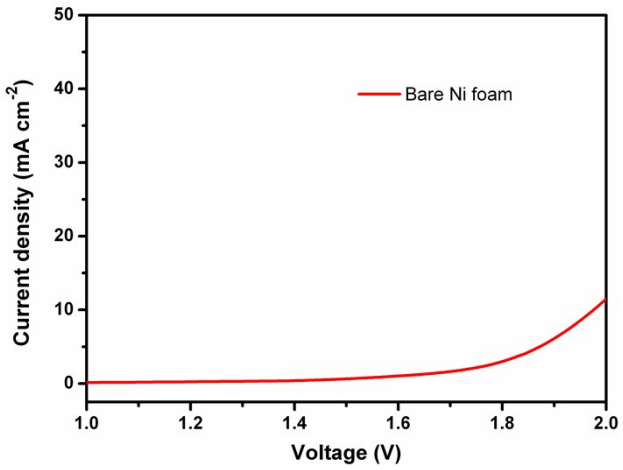

Fig. S19 LSV polarization curve of bare Nickel foam for overall water splitting.

Table S4 Comparison of the overall water splitting performance of the Ni/Ni_3C-NCNT 650-2 with other non-noble-metal catalysts in 1.0 M KOH solution.

Electrocatalysts	Potential (V) (j=10 mA cm^{-2})	Ref.
Ni/Ni_3C-NCNT 650-2	1.65	This work
$NiFe/NiCo_2O_4$/NF	1.67	[14]
Ni_3Se_2	1.64	[31]
PO-Ni/Ni-N-CNFs	1.69	[32]
NiFe HNSs	1.70	[33]
$NiCo_2O_4$ NW	1.63	[34]
$NiCo_2O_4$	1.65	[35]

$Ni_{11}(HPO_3)_8(OH)_6$	1.65	[36]
$Co_{24}Ni_1B_{75}$@NF	1.72	[37]
Ni_5P_4	1.70	[9]
Ni_3S_2	1.76	[10]
NiS	1.64	[12]

References

[1] X. Xiao, D. Huang, Y. Fu, M. Wen, X. Jiang, X. Lv, M. Li, L. Gao, S. Liu, M. Wang, C. Zhao, and Y. Shen, *ACS Appl. Mater. Interfaces*, 2018, **10**, 4689–4696.

[2] H. Jin, J. Wang, D. Su, Z. Wei, Z. Pang and Y. Wang, *J. Am. Chem. Soc.*, 2015, **137**, 2688–2694.

[3] C. G. Morales-Guio, L. Liardet, M. T. Mayer, S. D. Tilley, M. Grätzel and X. Hu, *Angew. Chem. Int. Ed.*, 2015, **54**, 664–667.

[4] J. Tian, Q. Liu, A. M. Asiri and X. Sun, *J. Am. Chem. Soc.*, 2014, **136**, 7587–7590.

[5] Y. Zhang, B. Yang, J. Xu, S. Chen, R. S. Rawat and H. Fan, *Adv. Energy Mater.*, 2016, **6**, 1600221.

[6] L. Jiao, Y. X. Zhou and H. L. Jiang, *Chem. Sci.*, 2016, **7**, 1690–1695.

[7] J. Luo, J. H. Im, M. T. Mayer, M. Schreier, M. K. Nazeeruddin, N. G. Park, S. D. Tilley, H. J. Fan and M. Grätzel, *Science*, 2014, **345**, 1593–1596.

[8] C. Y.Son, I. H. Kwak, Y. R. Lim and J. Park, *Chem. Commun.*, 2016, **52**, 2819–2822.

[9] M. Ledendecker, S. K. Calderýn, C. Papp, H. P. Steinrîck, M. Antonietti and M. Shalom, *Angew. Chem. Int. Ed.*, 2015, **54**, 12361–12365.

[10] L. L. Feng, G. Yu, Y. Wu, G. D. Li, H. Li, Y. Sun, T. Asefa, W. Chen and X. Zou, *J. Am. Chem. Soc.*, 2015, **137**, 14023–14026.

[11] C. Ouyang, X. Wang, C. Wang, X. Zhang, J. Wu, Z. Ma, S. Dou and S. Wang, *Electrochim. Acta*, 2015, **174**, 297–301.

[12] W. Zhu, X. Yue, W. Zhang, S. Yu, Y. Zhang, J. Wang and J. Wang, *Chem. Commun.*, 2016, **52**, 1486–1489.

[13] C. Xiao, Y. Li, X. Lu and C. Zhao, *Adv. Funct. Mater.*, 2016, **26**, 3515–3523.

[14] Q. Yan, H. Fan, H. Yu, Y. Zhang, Y. Zheng, Z. Dai, Y. Luo, B. Li and Y. Zong, *Angew. Chem.*, 2017, **129**, 12740–12744.

[15] X. Xu, X. Han, X. Ma, W. Zhang, Y. Deng, C. Zhong and W. Hu, *ACS Appl. Mater.*

Interfaces, 2017, **9**, 12574–12583.

[16] Z. Liu, H. Tan, J. Xin, J. Duan, X. Su, P. Hao, J. Xie, J. Zhan, J. Zhang, J. J. Wang and H. Liu, *ACS Appl. Mater. Interfaces*, 2018, **10**, 3699–3706.

[17] R. M. Yadav, J. Wu, R. Kochandra, L. Ma, C. S. Tiwary, L. Ge, G. Ye, R. Vajtai, J. Lou and P. M. Ajayan, *ACS Appl. Mater. Interfaces*, 2015, **7**, 11991–12000.

[18] Y. Zhao, R. Nakamura, K. Kamiya, S. Nakanishi and K. Hashimoto, *Nat. Commun.*, 2013, **4**, 2390.

[19] H. Liang, F. Meng, M. Cabán-Acevedo, L. Li, A. Forticaux, L. Xiu, Z. Wang and S. Jin, *Nano Lett.*, 2015, **15**, 1421–1427.

[20] B. Chen, X. He, F.Yin, H. Wang, D. J. Liu, R. Shi, J. Chen and H. Yin, *Adv. Funct. Mater.*, 2017, **27**, 1700795.

[21] H. Wang, Y. Cao, G. Zou, Q. Yi, J. Guo and L. Gao, *ACS Appl. Mater. Interfaces*, 2017, **9**, 60–64.

[22] Z. Y. Yu, Y. Duan, M. R. Gao, C. C. Lang, Y. R. Zheng and S. H. Yu, *Chem. Sci.*, 2017, **8**, 968–973.

[23] Y. Yang, K. Zhang, H. Lin, X. Li, H. C. Chan, L. Yang and Q. Gao, *ACS Catal.*, 2017, **7**, 2357–2366.

[24] Y. J. Tang, C. H. Liu, W. Huang, X. L. Wang, L. Z. Dong, S. L. Li and Y. Q. Lan, *ACS Appl. Mater. Interfaces*, 2017, **9**, 16977–16985.

[25] J. Landon, E. Demeter, N. İnoğlu, C. Keturakis, I. E. Wachs, R. Vasić, A. I. Frenkel and J. R. Kitchin, *ACS Catal.*, 2012, **2**, 1793–1801.

[26] H. Shi, and G. Zhao, *J. Phys. Chem. C*, 2014, **118**, 25939–25946.

[27] M. Gao, W. Sheng, Z. Zhuang, Q. Fang, S. Gu, J. Jiang and Y. Yan, *J. Am. Chem. Soc.*, 2014, **136**, 7077–7084.

[28] S. Klaus, Y. Cai, M. W. Louie, L. Trotochaud and A. T. Bell, *J. Phys. Chem. C*, 2015, **119**, 7243–7254.

[29] L. Kuai, J. Geng, C. Chen, E. Kan, Y. Liu, Q. Wang and B. Geng, *Angew. Chem. Int. Ed.*, 2014, **126**, 7677–7681.

[30] Q. Zhang, Y. Wang, Y. Wang, A. M. Al-Enizi, A. A. Elzatahry and G. *J.* Zheng, *Mater.*

Chem. A, 2016, **4**, 5713–5718.

[31] J. Shi, J. Hu, Y. Luo, X. Sun and A. M. Asir, *Catal. Sci. Technol.*, 2015, **5**, 4954–4958.

[32] Z. Y. Wu, W. B. Ji, B. C. Hu, H. W. Liang, X. X. Xu, Z. L. Yu, B. Y. Li and S. H. Yu, *Nano Energy*, 2018, **51**, 286–293.

[33] X. Sun, Q. Shao, Y. Pi, J. Guo and X. Huang, *J. Mater. Chem. A*, 2017, **5**, 7769–7775.

[34] S. Arumugam, G. Pandian and S. Sangaraju, *Adv. Funct. Mater.*, 2016, **26**, 4661–4672.

[35] X. Gao, H. Zhang, Q. Li, X. Yu, Z. Hong, X. Zhang, C. Liang and Z. Lin, *Angew. Chem. Int. Ed.*, 2016, **55**, 6290–6294.

[36] P. W. Menezes, C. Panda, S. Loos, F.Bunschei-Bruns, C. Walter, M. Schwarze, X. Deng, H. Dau, M. Driess, *Energy Environ. Sci.*, 2018, **11**, 1287–1298.

[37] N. Xu, G. Cao, Z. Chen, Q. Kang, H. Dai and P. Wang, *J. Mater. Chem. A*, 2017, **5**, 12379–12384.